Published in final edited form as:
Stem Cells. 2014 February ; 32(2): 414–423. doi:10.1002/stem.1569.

Loss of spastin function results in disease-specific axonal defects in human pluripotent stem cell-based models of hereditary spastic paraplegia

Kyle R. Denton[1], **Ling Lei**[1], **Jeremy Grenier**[1], **Vladimir Rodionov**[2], **Craig Blackstone**[3], and **Xue-Jun Li**[1,4,*]

[1]Department of Neuroscience, The University of Connecticut Health Center, Farmington, CT 06032, USA

[2]Center for Cell Analysis and Modeling and Department of Cell Biology, The University of Connecticut Health Center, Farmington, CT 06032, USA

[3]Cell Biology Section, Neurogenetics Branch, National Institute of Neurological Disorders and Stroke, National Institutes of Health, Bethesda, MD 20892, USA

[4]The Stem Cell Institute, The University of Connecticut Health Center, Farmington, CT 06032, USA

Abstract

Human neuronal models of hereditary spastic paraplegias (HSP) that recapitulate disease-specific axonal pathology hold the key to understanding why certain axons degenerate in patients and to developing therapies. SPG4, the most common form of HSP, is caused by autosomal dominant mutations in the *SPAST* gene, which encodes the microtubule-severing ATPase spastin. Here, we have generated a human neuronal model of SPG4 by establishing induced pluripotent stem cells (iPSCs) from an SPG4 patient and differentiating these cells into telencephalic glutamatergic neurons. The SPG4 neurons displayed a significant increase in axonal swellings, which stained strongly for mitochondria and tau, indicating the accumulation of axonal transport cargoes. In addition, mitochondrial transport was decreased in SPG4 neurons, revealing that these patient iPSC-derived neurons recapitulate disease-specific axonal phenotypes. Interestingly, spastin protein levels were significantly decreased in SPG4 neurons, supporting a haploinsufficiency mechanism. Furthermore, cortical neurons derived from spastin-knockdown human embryonic stem cells (hESCs) exhibited similar axonal swellings, confirming that the axonal defects can be caused by loss of spastin function. These spastin-knockdown hESCs serve as an additional model for studying HSP. Finally, levels of stabilized acetylated-tubulin were significantly increased in SPG4 neurons. Vinblastine, a microtubule-destabilizing drug, rescued this axonal swelling phenotype in neurons derived from both SPG4 iPSCs and spastin-knockdown hESCs. Thus, this

*Correspondence: Xue-Jun Li, PhD, Assistant Professor, Department of Neuroscience, Room E4029, MC-3401, The University of Connecticut Health Center, 263 Farmington Avenue, Farmington, CT 06030-3401, Tel: (860) 679-3026, Fax: (860) 679-8766, xjli@uchc.edu.

Competing interests statement: The authors declare that they have no competing financial interests.

Author Contribution Summary

Kyle R. Denton: Conception and design, data analysis and interpretation, manuscript writing
Ling Lei: Collection and assembly of data
Jeremy Grenier: Collection and assembly of data
Vladimir Rodionov: Data analysis and interpretation
Craig Blackstone: Provision of study material or patients, data analysis and interpretation
Xue-Jun Li: Conception and design, financial support, manuscript writing, data analysis and interpretation, final approval of manuscript

study demonstrates the successful establishment of human pluripotent stem cell-based neuronal models of SPG4, which will be valuable for dissecting the pathogenic cellular mechanisms and screening compounds to rescue the axonal degeneration in HSP.

Keywords

iPSCs; hESCs; spastin; hereditary spastic paraplegia; axonal degeneration; RNA interference

Introduction

Hereditary spastic paraplegias (HSP) are a heterogeneous group of genetic disorders that result in progressive lower limb spasticity [1]. The symptoms are due to a length-dependent axonopathy, most severely affecting corticospinal motor neurons (CSMN). These neurons display a “dying back” axonopathy, particularly in the spinal cord, resulting in impaired lower motor neuron function which produces prominent lower limb spasticity and typically more mild weakness. Although there are 57 distinct genetic loci associated with HSP, SPG4 is the most common, accounting for nearly 40% of all cases of autosomal dominant HSP [2]. SPG4 is caused by mutations in the *SPAST* gene, which encodes the microtubule-severing ATPase spastin [2–5]. Spastin is a member of the ATPase associated with diverse cellular activities (AAA) family that also includes the microtubule-severing protein p60 katanin. The large variety of mutation types present in the *SPAST* gene of SPG4 patients has led to different hypotheses for the pathogenic mechanism of these mutations. The majority are nonsense mutations, deletions, or splice-site mutations. These are believed to reduce the amount of spastin present in a cell, causing disease through a haploinsufficiency mechanism [6]. This seems to be true for the majority of cases; however, there are certain missense mutations in the AAA ATPase domain that appear to act in a dominant-negative, loss-of-function fashion [7], which is possible because spastin functions as a hexamer [8]. Spastin is involved in a variety of functions, including microtubule dynamics [9], membrane remodeling [10], cytokinesis [10, 11], neurite outgrowth [12], and axonal transport [13–16].

A common observation researchers have made while studying SPG4 is that spastin affects microtubule-based transport. This fits with the role spastin plays in microtubule severing, as microtubule arrays are present through the entire length of axons and both provide structural support and serve as the railways for organelle transport. Axonal transport deficits also neatly match the observation that only the longest projection neurons are affected, since they would put the largest strain on transport systems to deliver cellular contents to the most distal portions of the cell. If materials are not properly delivered to the distal regions, it could cause a dying-back degeneration of the axon, as seen in HSP. Some of the best lines of evidence linking spastin and transport come from two different HSP mouse models that possess different spastin mutations [14, 16]. These studies showed that cortical neurons cultured *in vitro* could be used to model axonal defects, although the mechanisms underlying the axonal defects in SPG4 remain largely unknown.

To date, the role of spastin has not been investigated in human cortical neurons, but the advent of induced pluripotent stem cell technology [17, 18] now provides researchers with a system for studying the specific cell types that are affected by various diseases in vitro. This method has been employed for several neurodegenerative disorders including spinal muscular atrophy [19], amyotrophic lateral sclerosis [20], Parkinson disease [21], and Huntington disease [22]. Here, we for the first time generated human iPSCs from an SPG4 patient as well as spastin knockdown hESCs to model HSP. The generated human pluripotent stem cell (hPSC) lines serve as a renewable source of cells that can be differentiated into forebrain projection neurons, which include the most severely affected

corticospinal motor neurons in HSP. In neurons generated from SPG4 iPSC lines, we observed an increase in the number of axonal swellings and accumulation of mitochondria within these regions, leading us to quantify fast axonal transport. This revealed a significant decrease in the number of motile mitochondria in the SPG4-derived neurons, and decreased motile events in the retrograde direction. It appears as if these defects were due to spastin haploinsufficiency, as the level of spastin protein was significantly decreased in the SPG4-derived neurons. To confirm that loss of spastin function is implicated in the pathogenesis of SPG4, we examined spastin knockdown neurons, and found a similar increase in axonal swellings. Lastly, to show that these cells will be useful as a drug screening platform, we treated iPSC-derived and spastin knockdown neurons with the microtubule-destabilizing drug vinblastine. This treatment led to a significant reduction in axonal swellings as compared to vehicle-treated cells. These findings suggest that these hPSC-based models of SPG4 will serve as a useful model for HSP, since no therapies exist that can prevent, slow the progression, or cure HSP.

Materials and Methods

Reprogramming human fibroblasts into iPSC lines

Human iPSC lines were established from human fibroblasts by transfecting them with excisable lentiviruses (kindly provided by Dr. Gustavo Mostoslavsky) [23, 24] or episomal plasmids (Addgene), as reported previously [25]. Briefly, human fibroblasts collected under an IRB-approved clinical protocol (NINDS protocol 00-N-0043) at the NIH Clinical Center were seeded at ~10^5 cells/ 35-mm dish in DMEM supplemented with 10% fetal bovine serum (FBS) and 0.1 mM non-essential amino acids. For lentiviral infection, cells were infected with EF1α-hSTEMCCA-loxP lentiviruses containing pluripotency genes (Oct4, Sox2, c-Myc, Klf4). For episomal transduction, human fibroblasts (~200,000) were dissociated and then infected with episomal plasmids containing pluripotency factors (Oct3/4, Sox2, L-Myc, Klf4, and Lin 28). At around 1 week after lentiviral infection or electroporation transduction, cells were plated onto a 35-mm dish in DMEM supplemented with 10% FBS. After culturing for 7 days, cells were dissociated and seeded onto mouse embryonic fibroblast (MEF) feeder at ~10^5 cells/100-mm dish. Two weeks later, colonies with morphologies similar to hESCs were observed. These colonies were split onto MEF feeder cells to derive iPSC lines. After several passages, homogenous colonies with ESC-like morphology were generated. The lentiviral iPSC lines used in this study were iWT-l1, iSPG4-l4, and iSPG4-l7. The episomal iPSC lines used in this study were iWT-e1, iWT-e3, iSPG4-e6, and iSPG4-e8.

Lentivirus production and transduction of hESCs

To produce high-titer lentivirus, 10 μg of lentiviral transfer vector (pLVTHM), 7.5 μg of lentiviral vector psPAX2, and 5 μg of pMD2.G (VSV-G envelope protein) were cotransfected into HEK293FT cells (Invitrogen) using the calcium phosphate method. Sixty hours after transfection, cell culture medium containing viral particles was collected and filtered through a 0.45-μm filter (Millipore). Viral particles were further concentrated by ultracentrifugation (SW 28 rotor, Beckman) at 50,000 g for 2 h, and the pellet was resuspended in hESC medium. For transduction of ESCs, hESCs were passaged normally and pelleted by brief centrifugation. Cell pellets were then incubated with 100 μl of concentrated virus (10^6 transducing units/ml) at 37°C for 30 min. To knock down spastin, pLVTHM lentiviruses contain shRNA targeting spastin or luciferase (as control) were used to infect hESCs, a strategy similar to that we have used for knocking down other genes [26]. RNAi hESCs were expanded and then differentiated as described below.

hPSC Neural Differentiation

To generate telencephalic projection neurons from hPSCs, stem cells were cultured on a feeder layer of irradiated MEFs in 6-well tissue culture treated plates for around 6 days, with the hESC media (+10μg/ml FGF-2) changed daily. When almost confluent, cells were detached from the feeder layer to initiate the neural differentiation, as we previously described [27–29]. The cells were cultured in suspension for 4 days in hESC media, changing the media every day. On day 5, neural induction was started by transferring the generated PSC aggregates to neural induction media (NIM). After 3 additional days in suspension, PSC aggregates were plated onto 6-well tissue culture treated plates in NIM with 10% FBS. After 12 hours, the media was changed with fresh NIM. The media was then changed every other day until day 17, when the generated neuroepithelial (NE) cells were isolated. Mechanically-isolated NE cells were cultured in suspension with NIM (+B27, +cyclic AMP, +insulin-like growth factor 1 [IGF1]) to generate neurospheres for at least an additional 10 days. On about day 28, the neurospheres were dissociated and plated onto polyornithine- and laminin-coated coverslips in neural differentiation media (NDM) containing N2, B27, ascorbic acid, cyclic AMP, laminin, IGF1, brain-derived neurotrophic factor, and glial-derived neurotrophic factor. Half of the media was changed every other day for a total of 6 to 12 weeks, depending on the analysis to be performed. To treat cells with vinblastine, the media was replaced with standard NDM with 10 nM vinblastine (Sigma-Aldrich) dissolved in water.

Immunocytochemistry

Cells on glass coverslips are fixed with 4% paraformaldehyde for 20 minutes. A 0.2% Triton-X solution was used to permeabilize the cells for 10 minutes followed by several PBS washes. The samples are incubated in a primary antibody solution overnight. On the following day, samples are incubated with the appropriate secondary antibody for 30 minutes [28]. To quantify axonal swellings, at least three blindly-selected fields were imaged for at least three coverslips per group. The number of axonal swellings were counted and divided by the total length of Tau^+ axons in each field, which were measured using MetaMorph software.

Antibodies

Mouse IgM anti-Tra-1-60 (Santa Cruz, 1:50), goat IgG anti-Nanog (R&D, 1:500), mouse IgG3 anti-SSEA-4 (DSHB, 1:100), mouse IgG anti-acetylated tubulin (Sigma-Aldrich, 1:10,000), rabbit IgG anti-Tau (Sigma-Aldrich, 1:100), rat IgG_{2a} anti-GFP (Nacalai Tesque, 1:1000), rabbit IgG anti-Tbr1 (Proteintech, 1:1,000), βIII-tubulin, mouse IgG (DSHB, 1:100).

Reverse transcriptase Polymerase Chain Reaction (RT-PCR)

RNA was isolated from cells using TRIzol reagent (Invitrogen) following manufacturer's instructions. A total of 2μg of RNA was used to synthesize cDNA using iScriptcDNA Synthesis Kit (Bio-Rad) following manufacturer's parameters: 5 min @ 25°C, 30 min @ 42°C, and 5 min @ 85°C. Semi-quantitative analysis was performed using RT-PCR with GoTaq Green Master Mix (Promega).

Western Blotting

We used a general protocol that was described previously [30]. A mouse monoclonal anti-spastin antibody (Sigma-Aldrich, 1:1000) was used to detect expression of spastin isoforms, and a mouse monoclonal anti-actin antibody (Sigma-Aldrich, 1:1000) was used as a loading control. The quantification of Western blotting was quantified using ImageJ [31] normalized against actin as a loading control.

Live Cell Imaging with MitoTracker

Neurospheres are plated onto polyornithine and laminin coated 35mm dishes (MatTek). At 8 weeks of total differentiation, the cells are stained with 50 nM MitoTracker Red CMXRos (Invitrogen) for 3 minutes to allow visualization of mitochondria and then the media is replaced with fresh NDM. Live-cell imaging was performed using a Carl Zeiss Axiovert 200M microscope equipped with an incubation chamber. The cells are kept at 37°C with 5% CO_2 while imaging. Axons identified according to morphological criteria (constant thin diameter, long neurites, no branching and direct emergence from the cell body) were imaged every 5 seconds for 5 minutes, yielding 60 frames. Quantifications were performed using the same protocol as described previously [32]. In short, the location of each mitochondrion was manually selected using the Track Points function in MetaMorph, and parameters such as distance from cell body and velocity were recorded. A velocity threshold of 300 nm/s was used to select microtubule based transport events [33]. To determine the percentage of motile mitochondria, the total number of mitochondria that were present along the imaged neurite was counted, and those that changed position (velocity >300 nm/s) in at least 3 consecutive frames were considered motile.

Statistical analysis

The statistical significance in mean values among multiple sample groups was analyzed with Turkey's studentized range test after ANOVA. Two-sided *t*-test was used to examine the statistical significance between two sample groups. The trend between knockdown efficiency and increased swellings was tested using linear regression analysis. The significance level was defined as $p < 0.05$, and all significance tests were conducted using SAS 9.1 (SAS Institute).

Results

Characterization and differentiation of control and SPG4 iPSC lines

SPG4 iPSCs were generated from dermal fibroblasts of an SPG4 patient with a heterozygous G>T substitution located in intron 4 of the *SPAST* gene that alters the splice acceptor site (c. 683-1G>T). The fibroblasts were reprogrammed to iPSCs using both a lentiviral [23, 34] and an episomal method [25], which permitted us to determine if the reprogramming method has any effect on the mutant phenotypes that we observe in the SPG4 neurons. Human iPSC lines derived from normal individuals were also generated and utilized as controls. All of the clones that we analyzed, from SPG4 and controls (wild-type [WT]), displayed characteristic colony morphology and stained positive for the pluripotency markers Nanog, Tra-1-60, and SSEA4 (Fig. 1A). The expression of pluripotency genes was analyzed by RT-PCR (Fig. 1B); only in the iPSCs was expression of Sox2, Nanog, or Oct4 detected. Teratomas were generated in mice using the iPSC lines to confirm that they were pluripotent. Both the lentiviral and episomal iPSC lines were able to spontaneously differentiate into tissues of each of the three germ layers, confirming pluripotency (Fig. 1C). The region surrounding the splice acceptor site of intron 4 was sequenced to confirm that the SPG4-derived iPSC lines maintained the mutation in the *SPAST* gene after reprogramming (Fig. 1D). Because it is known that iPSCs are susceptible to chromosomal abnormalities after passaging, karyotype analysis was performed, which did not reveal any defects (Fig. 1E).

Next, the iPSC lines were differentiated to the neural lineage to generate forebrain glutamatergic neurons using a protocol we established previously, which leads to the efficient generation of telencephalic neurons [27–29]. Both control and SPG4 iPSCs efficiently differentiated into neurons with long processes, regardless of the reprogramming method (Fig. 1F). These neurons were $Tbr1^+$, confirming that they are glutamatergic (Fig. 1F). There were no significant differences in the percentages of $Tbr1^+$ cells between control

and SPG4 cells (Fig. 1G). Since the spastin mutation in this SPG4 patient would affect RNA splicing, we performed western blot analysis to examine the levels of spastin present in neurons generated from the iPSCs. Our data showed a reduction in spastin protein levels in the neurons derived from the SPG4 patient lines as compared to controls (~47% of control; Fig. 1H). Since SPG4 is caused by autosomal dominant mutations, SPG4 patients likely have ~50% of spastin activity if one allele is nonfunctional. Thus, the SPG4 iPSC-derived neurons track level of spastin expected in patients, providing a unique model to study the pathological changes caused by reduced spastin levels.

Neurons derived from SPG4 iPSCs exhibit increased axonal swellings

A common pathologic hallmark of SPG4 is the enlargement of axons that accumulate organelles, termed axonal swellings [14]. To determine if the iPSC-derived neurons displayed axonal phenotypes similar to that observed in post mortem spinal cord sections, we performed acetylated tubulin staining to examine the formation of axonal swellings (Fig. 2A). Our analysis showed that there was a substantial increase in the number of axonal swellings in the SPG4-derived neurons as compared to controls (Fig. 2B). Furthermore, the axons with swellings in SPG4 neurons were significantly longer than those without (SPG4 axons without swellings = 53.16±2.88 μm vs. those with swellings = 93.04±5.87 μm; $p<0.01$), suggesting that longer axons were more susceptible to these changes. Similar swellings were present in the neurons derived from the episomal SPG4 iPSC lines, indicating that the reprogramming method did not affect this phenotype (Fig. 2C). It is plausible that reduced levels of a microtubule-severing enzyme, like spastin, would lead to increased microtubule stability. To test this, we performed Western analysis for stabilized microtubules in extracts from week 6 iPSC-derived neurons, using an acetylated tubulin antibody. This revealed a dramatic increase in acetylated tubulin levels in the SPG4 patient-derived neurons as compared to controls (Fig. 2D).

Fast axonal transport of mitochondria is disrupted in SPG4 neurons

Axonal swellings have been associated with the accumulation of transported cargos [14, 16], indicating that axonal transport may be impaired. To assess axonal transport in SPG4 iPSC-derived cortical neurons, we performed immunostaining for mitochondria and acetylated tubulin. This revealed the accumulation of mitochondrial staining within axonal swellings (Fig. 3A), suggesting impaired transport of these organelles. To further analyze mitochondrial fast axonal transport, live cell imaging was performed on week 8 control and SPG4-derived neurons. Images of axons were taken every 5 seconds for 5 minutes. As shown in representative kymographs of mitochondria within proximal axons (Fig. 3B), a significant decrease in the mitochondrial movement (indicated along the X-axis) was observed in neurons derived from SPG4 iPSCs. Further analysis of individual trajectories of each mitochondria revealed a significant reduction in the percentage of motile mitochondria; in control iPSC-derived neurons, 10.5% of the mitochondria were motile, compared to just 3.4% in the SPG4-derived neurons (Fig. 3C). Transport vesicles and membranous organelles move along a polarized array of cytoplasmic microtubules down the axon (anterograde transport) and back to the cell body (retrograde transport). It remains unclear whether anterograde or retrograde transport is affected in SPG4. Therefore, using these patient iPSC-derived neurons, we further analyzed the velocity of motile mitochondria and frequency of motile movements in both the anterograde and retrograde directions (Table 1). The mitochondrial transport velocity in both anterograde and retrograde direction did not differ between control and SPG4 neurons, suggesting that the ATPase activity of the molecular motors was unaffected. Next, the frequency of fast axonal transport events was calculated; there was a 68% reduction in the frequency of motile events in the SPG4-derived neurons as compared to controls. Subdivision into anterograde and retrograde events revealed a directional selectivity in the effect of reduced spastin activity on fast axonal transport. While

the number of anterograde events above the velocity threshold was not significantly different between control and SPG4 cells (though there was a trend toward reduction), there was a prominent 80% reduction in the number of retrograde events in the SPG4 cells, implicating retrograde axonal transport in SPG4 pathogenesis.

Knocking down spastin leads to axonal defects similar to those in SPG4-derived neurons

Considering that SPG4 iPSC-derived neurons recapitulate the disease-specific phenotypes and that the spastin protein is significantly reduced in these neurons, the axonal defects in SPG4 may result from loss of spastin function. To test this, we established spastin-knockdown hESC lines using lentiviral infection of shRNA constructs (Fig. 4A). To minimize off-target effects, two shRNAs targeted against different regions of spastin were cloned into the pLVTHM lentiviral vector that allows for the simultaneous expression of GFP and shRNA. After infecting H9 hESCs with the corresponding lentivirus, GFP^+ cells were selected to obtain a pure population of knockdown cells (Fig. 4B). The spastin knockdown hESCs, as well as the control luciferase RNAi hESCs, were differentiated to the neural lineage and glutamatergic neurons as we described for SPG4 iPSCs. Expression of the shRNA was maintained during neural differentiation, as GFP was robustly expressed (Fig. 4B). To confirm the knockdown efficiency of the shRNA constructs, Western analysis was performed on cells at the hESC stage and in differentiated neurons (Fig. 4C). In day 40 neurons, there was around 40% and 77% knockdown of spastin protein level in the spastin RNAi lines 1 and 2, respectively. Notably, when the morphology of the neurons was examined, axonal swellings were prominent in neurons from the two spastin knockdown lines (Fig. 4D). Quantification revealed a significant increase in the number of swellings in the cells with reduced spastin as compared to controls (Fig. 4E). Interestingly, there was a trend toward increased swellings, with the higher knockdown efficiency ($p<0.01$ by linear regression analysis). These data confirm that loss of spastin function results in the disease-specific axonal pathological changes in hPSC-derived neurons.

Microtubule-destabilizing drug rescues the axonal swelling phenotype

In order to show that the cells generated in this study have utility in screening for potential therapeutic compounds, we treated SPG4 iPSC-derived neurons and spastin knockdown hESC-derived neurons with the microtubule-destabilizing drug vinblastine. Vinblastine has been shown to be efficacious at reducing axonal swellings in $SPG4^{\Delta/\Delta}$ primary mouse neurons [13], increasing the cell body size of olfactory neural progenitors from SPG4 patients [35], and ameliorating the neurodegenerative phenotypes in *Drosophila* [36]. When week 8 iSPG4-l7 neurons were treated with 10 nM vinblastine for just 24 hours, there appeared to be a reduction in the number of axonal swellings (Fig. 5A), and quantification confirmed that vinblastine significantly reduced the number of axonal swellings in these cells (Fig. 5B). To confirm the protective effect of vinblastine against axonal defects in human neurons, we treated week 10 spastin knockdown neurons with vinblastine (Fig. 5C). Similar to the iPSC-derived neurons, vinblastine treatment significantly reduced the number of axonal swellings (Fig. 5D). Taken together, our data revealed that nanomolar concentration of the microtubule-destabilizing drug vinblastine can ameliorate the axonal defects observed in this human neuronal model of SPG4. This implicates disorganization of microtubules in the axonal phenotypes of SPG4.

Discussion

Human pluripotent stem cells, including hESCs and iPSCs, can differentiate into any cell type in the body, including neurons. Based on developmental principles, different neuronal subtypes have been generated using *in vitro* differentiation protocols. Using these systems, PSCs have been used to model several neurogenetic disorders [19, 22, 37–45], via

genetically modifying hESCs or using patient-specific iPSCs and then differentiating these stem cells into the neurons affected by a particular disease. Here, we have differentiated SPG4 iPSCs and spastin-knockdown hESCs to forebrain projection neurons in order to model HSP. We generated iPSCs from an SPG4 patient who possesses a heterozygous mutation (c.683-1G>T) that affects mRNA splicing, resulting in a reduction in spastin levels. Neurons from these lines had a significant increase in axonal swellings which appeared to accumulate mitochondria, suggesting altered axonal transport in these regions. Analysis of fast axonal transport of mitochondria revealed a significant decrease in the percentage of motile mitochondria and a decrease in the frequency of motile events, particularly in the retrograde direction. To confirm that spastin loss-of-function is responsible for these findings, we generated spastin knockdown lines. Similarly, a significant increase in axonal swellings was found in the knockdown cells compared to a control knockdown line. Moreover, it appeared that cells with the greater reduction in spastin levels exhibited that largest increase in swellings. In addition, the protein expression of stable acetylated tubulin was increased in SPG4 neurons. Treatment with the microtubule-destabilizing drug vinblastine was able to rescue the axonal swelling phenotype in SPG4 and spastin-knockdown neurons. To our knowledge, this is the first study to recapitulate the axonal defects of HSP in human neurons. Our study also implicates the loss of spastin function and subsequent disruption in microtubule organization in the axonal defects in SPG4 neurons.

Our results support the hypothesis that spastin loss-of-function is responsible for mediating disease in SPG4 patients. There was a dramatic decrease in spastin levels in the neurons generated from the SPG4 iPSC lines as compared to lines from control individuals. In addition, SPG4-derived neurons with reduced spastin displayed a significant increase in axonal swellings. Interestingly, the axons that possessed swellings were significantly longer than those without, suggesting that the longer axons may be more susceptible to defects caused by reduced spastin levels. This is concordant with the length-dependent degeneration of the longest CSMN axons in SPG4. Notably, we were able to observe a similar increase in swellings in neurons from spastin knockdown lines, suggesting that this phenotype was dependent on spastin dosage. The presence of axonal swellings in our system, at as early as 6 weeks of differentiation, is very interesting. Neurons at this stage are comparable to immature fetal cells [46], suggesting that defects in patient cells may be present prior to the onset of symptoms. An alternative explanation for this may be the inherent differences in the *in vitro* environment compared to *in vivo* environment, which may affect the onset and severity of the phenotype. Our findings are in agreement with the published studies of two SPG4 mouse models, where a reduction in spastin also led to phenotypes similar to HSP patients and axonal swellings in cortical neurons [14, 16]. Although the knockout mice only had minor motor deficits compared to those of HSP patients, perhaps the prominent differences in absolute size of CSMNs in mice and humans can account for this. One of the difficulties in examining CSMNs using *in vitro* cultures is the lack of a specific marker, and a directed differentiation method that specifically generates CSMNs is currently unavailable. However, the differentiation method used in this study can produce neurons that express factors enriched in these cells [28], such as FezF2 and Ctip2 [47]. In the future, if conditions for specifying CSMNs are established, it would be interesting to determine whether these neurons are more susceptible to axonal swellings than other neuronal subtypes.

Microtubules are a major component of the neuronal cytoskeleton, and they are needed for the extension of neurites in developing neurons and to serve as railways for cargo transport in mature neurons [48, 49]. They are composed of α- and β-tubulin heterodimers that are selectively arranged in axons so that the plus-end is oriented distal to the soma. All forms of α-tubulin can be acetylated at Lys40, while β-tubulin is not. Long-lived, stable microtubules are enriched in acetylated tubulin [50], particularly in the proximal portion of axons [51].

Although the exact role of tubulin acetylation has not been fully resolved, studies on Huntington and Parkinson disease models have reported that altered levels of acetylated tubulin result in axonal transport deficits [52, 53]. We found that levels of acetylated tubulin were dramatically increased in SPG4-derived week 6 neurons compared to control neurons. Reduction in the microtubule-severing activity of spastin in the SPG4-derived neurons would be expected to cause such an increase in stabilized microtubules. This result is contrary to what was observed in olfactory neurosphere-derived cells isolated from SPG4 patients [35], where a decrease in acetylated tubulin in SPG4 cells was reported to reflect an increased expression of the microtubule-destabilizing protein stathmin. Differences in the cell types that were analyzed between these two studies may account for the opposing changes in acetylated tubulin levels. This further suggests that differentiating cells to mature neurons that possess axons may be important for recapitulating disease-specific abnormalities.

Deficits in axonal transport are a common observation among different forms of neurodegenerative disorders. This is not surprising, since the axoplasm accounts for >99% of total cellular volume in the longest neurons, which puts enormous strain on the intracellular transport mechanisms needed to traffic proteins, lipids, and other molecules to and from the most distal parts of the cell [54]. Microtubule-severing enzymes are involved in generating the diverse array of microtubules present in axons [55]. As revealed in our study, levels of acetylated tubulin were significantly increased in SPG4 neural cultures. In $Sp^{\Delta/\Delta}$ mice, loss of spastin leads to a decrease in dynamic microtubule ends, and an increase in detyrosinated, stable microtubules along axonal swellings [16]. These changes can lead to alterations in microtubule-associated protein (MAP), kinesin, and dynein binding [48]. The decrease in motile mitochondria we observed in SPG4-derived neurons supports a pathogenic role for disrupted microtubule-based transport in SPG4. Moreover, although the velocity of fast axonal transport was not altered, the frequency of motile events in the retrograde direction in particular was significantly decreased. Importantly, longer-lived, stable microtubules that are subjected to post-translational modifications and MAP binding may interfere with the binding of molecular motors, altering the frequency of motility events [56]. Retrograde axonal transport is important for bringing distal trophic factors or stress stimuli to the soma so that the neuron can respond properly [57]. Our finding agrees with a recent report on an SGP4 mouse model, $Sp^{\Delta}/^{\Delta}$, where retrograde transport was also specifically affected in neurons that lack spastin [13]. Moreover, fast axonal transport deficits are implicated in other related neurodegenerative diseases. For example, mutations in subunits of cytoplasmic dynein, a motor protein involved in retrograde transport, can result in motor neuron degeneration, suggesting that retrograde fast axonal deficits are sufficient to cause neurodegeneration [58, 59].

In the future, these SPG4 iPSCs should prove valuable in further unraveling the mechanisms of axonal degeneration in HSP. Understanding the link between microtubule defects found in SPG4 and other forms of HSP will be valuable in understanding the pathways required for axonal maintenance. A better notion of the pathways that spastin regulates will be useful in the development of therapies that may be applicable to multiple forms of HSP. This includes the other forms that are involved in ER morphogenesis: SPG3A, SPG12, and SPG31 [60–62]. In addition, this hPSC model of HSP will also be a valuable tool in testing future therapeutic strategies. The ability to examine the effects of drugs on the human cell types that are affected by disease is one of the main benefits of using hPSCs. This is particularly important since over 90% of CNS therapies fail during clinical trials, in part because of the lack of accurate models during preclinical stages [46, 63]. The evidence that vinblastine is capable of reducing axonal swellings in human cortical neurons shows that this system will be useful in the future for screening therapeutic agents to rescue axonal degeneration in HSP.

Conclusion

In this study, we have demonstrated the successful establishment of human neuronal models of SPG4 by generating both SPG4 patient-iPSCs and spastin-knockdown hESCs, and then differentiating these stem cells into telencephalic glutamatergic neurons. These hPSC-derived neurons displayed increased axonal swellings, accumulation of transported cargoes, and impaired mitochondrial transport, recapitulating disease-specific axonal phenotypes. To our knowledge, this is the first evidence of axonal transport deficits in human SPG4 neurons. Moreover, our data support the hypothesis that axonal phenotypes in SPG4 are caused by loss of spastin function, which is buttressed by both the decreased expression level of spastin in SPG4 iPSC-derived neurons and the observation of similar axonal phenotypes in spastin-knockdown neurons. Finally, the expression of stable acetylated-tubulin was increased in SPG4 neurons, and vinblastine, a microtubule-destabilizing drug, rescued the axonal swelling phenotype. These findings suggest that microtubules can be a potential therapeutic target for HSP in human neurons and our hPSC-based models of HSP serve as a unique paradigm to study the pathogenic mechanisms and to screen for therapeutic drugs.

Acknowledgments

We are grateful to Dr. Ricardo Roda for performing the skin biopsies. We also thank Dr. Gustavo Mostoslavsky for generously providing the lentiviral reprogramming vector. This study was supported by a Connecticut Stem Cell Research Grant (11SCB24) and the Spastic Paraplegia Foundation. V.R. was supported by NIH grant GM62290. C.B. was supported by the Intramural Research Program of the NINDS, National Institutes of Health.

References

1. Fink JK. Hereditary spastic paraplegia. Neurol Clin. 2002; 20(3):711–726. [PubMed: 12432827]
2. Hazan J, Fonknechten N, Mavel D, et al. Spastin, a new AAA protein, is altered in the most frequent form of autosomal dominant spastic paraplegia. Nat Genet. 1999; 23(3):296–303. [PubMed: 10610178]
3. Evans KJ, Gomes ER, Reisenweber SM, et al. Linking axonal degeneration to microtubule remodeling by Spastin-mediated microtubule severing. J Cell Biol. 2005; 168(4):599–606. [PubMed: 15716377]
4. Roll-Mecak A, Vale RD. The Drosophila homologue of the hereditary spastic paraplegia protein, spastin, severs and disassembles microtubules. Curr Biol. 2005; 15(7):650–655. [PubMed: 15823537]
5. Salinas S, Carazo-Salas RE, Proukakis C, et al. Human spastin has multiple microtubule-related functions. J Neurochem. 2005; 95(5):1411–1420. [PubMed: 16219033]
6. Lumb JH, Connell JW, Allison R, et al. The AAA ATPase spastin links microtubule severing to membrane modelling. Biochim Biophys Acta. 2012; 1823(1):192–197. [PubMed: 21888932]
7. Solowska JM, Garbern JY, Baas PW. Evaluation of loss of function as an explanation for SPG4-based hereditary spastic paraplegia. Hum Mol Genet. 2010; 19(14):2767–2779. [PubMed: 20430936]
8. Pantakani DV, Swapna LS, Srinivasan N, et al. Spastin oligomerizes into a hexamer and the mutant spastin (E442Q) redistribute the wild-type spastin into filamentous microtubule. J Neurochem. 2008; 106(2):613–624. [PubMed: 18410514]
9. Errico A, Ballabio A, Rugarli EI. Spastin, the protein mutated in autosomal dominant hereditary spastic paraplegia, is involved in microtubule dynamics. Hum Mol Genet. 2002; 11(2):153–163. [PubMed: 11809724]
10. Connell JW, Lindon C, Luzio JP, et al. Spastin couples microtubule severing to membrane traffic in completion of cytokinesis and secretion. Traffic. 2009; 10(1):42–56. [PubMed: 19000169]

11. Yang D, Rismanchi N, Renvoise B, et al. Structural basis for midbody targeting of spastin by the ESCRT-III protein CHMP1B. Nat Struct Mol Biol. 2008; 15(12):1278–1286. [PubMed: 18997780]
12. Yu W, Qiang L, Solowska JM, et al. The microtubule-severing proteins spastin and katanin participate differently in the formation of axonal branches. Mol Biol Cell. 2008; 19(4):1485–1498. [PubMed: 18234839]
13. Fassier C, Tarrade A, Peris L, et al. Microtubule-targeting drugs rescue axonal swellings in cortical neurons from spastin knockout mice. Dis Model Mech. 2012
14. Kasher PR, De Vos KJ, Wharton SB, et al. Direct evidence for axonal transport defects in a novel mouse model of mutant spastin-induced hereditary spastic paraplegia (HSP) and human HSP patients. J Neurochem. 2009; 110(1):34–44. [PubMed: 19453301]
15. Solowska JM, Morfini G, Falnikar A, et al. Quantitative and functional analyses of spastin in the nervous system: implications for hereditary spastic paraplegia. J Neurosci. 2008; 28(9):2147–2157. [PubMed: 18305248]
16. Tarrade A, Fassier C, Courageot S, et al. A mutation of spastin is responsible for swellings and impairment of transport in a region of axon characterized by changes in microtubule composition. Hum Mol Genet. 2006; 15(24):3544–3558. [PubMed: 17101632]
17. Takahashi K, Tanabe K, Ohnuki M, et al. Induction of pluripotent stem cells from adult human fibroblasts by defined factors. Cell. 2007; 131(5):861–872. [PubMed: 18035408]
18. Yu J, Vodyanik MA, Smuga-Otto K, et al. Induced pluripotent stem cell lines derived from human somatic cells. Science. 2007; 318(5858):1917–1920. [PubMed: 18029452]
19. Ebert AD, Yu J, Rose FF Jr, et al. Induced pluripotent stem cells from a spinal muscular atrophy patient. Nature. 2009; 457(7227):277–280. [PubMed: 19098894]
20. Weimann JM, Zhang YA, Levin ME, et al. Cortical neurons require Otx1 for the refinement of exuberant axonal projections to subcortical targets. Neuron. 1999; 24(4):819–831. [PubMed: 10624946]
21. Azim E, Shnider SJ, Cederquist GY, et al. Lmo4 and Clim1 progressively delineate cortical projection neuron subtypes during development. Cereb Cortex. 2009; 19(Suppl 1):i62–69. [PubMed: 19366868]
22. Zhang N, An MC, Montoro D, et al. Characterization of Human Huntington's Disease Cell Model from Induced Pluripotent Stem Cells. PLoS Curr. 2010; 2:RRN1193. [PubMed: 21037797]
23. Somers A, Jean JC, Sommer CA, et al. Generation of transgene-free lung disease-specific human induced pluripotent stem cells using a single excisable lentiviral stem cell cassette. Stem Cells. 2010; 28(10):1728–1740. [PubMed: 20715179]
24. Sommer CA, Sommer AG, Longmire TA, et al. Excision of reprogramming transgenes improves the differentiation potential of iPS cells generated with a single excisable vector. Stem Cells. 2010; 28(1):64–74. [PubMed: 19904830]
25. Okita K, Matsumura Y, Sato Y, et al. A more efficient method to generate integration-free human iPS cells. Nat Methods. 2011; 8(5):409–412. [PubMed: 21460823]
26. Wang ZB, Zhang X, Li XJ. Recapitulation of spinal motor neuron-specific disease phenotypes in a human cell model of spinal muscular atrophy. Cell Res. 2013; 23(3):378–393. [PubMed: 23208423]
27. Boisvert EM, Denton K, Lei L, et al. The specification of telencephalic glutamatergic neurons from human pluripotent stem cells. J Vis Exp. 2013; (74)
28. Li XJ, Zhang X, Johnson MA, et al. Coordination of sonic hedgehog and Wnt signaling determines ventral and dorsal telencephalic neuron types from human embryonic stem cells. Development. 2009; 136(23):4055–4063. [PubMed: 19906872]
29. Zeng H, Guo M, Martins-Taylor K, et al. Specification of region-specific neurons including forebrain glutamatergic neurons from human induced pluripotent stem cells. PLoS One. 2010; 5(7):e11853. [PubMed: 20686615]
30. Wang ZB, Zhang X, Li XJ. Recapitulation of spinal motor neuron-specific disease phenotypes in a human cell model of spinal muscular atrophy. Cell Res. 2012
31. Schneider CA, Rasband WS, Eliceiri KW. NIH Image to ImageJ: 25 years of image analysis. Nat Methods. 2012; 9(7):671–675. [PubMed: 22930834]

32. De Vos KJ, Chapman AL, Tennant ME, et al. Familial amyotrophic lateral sclerosis-linked SOD1 mutants perturb fast axonal transport to reduce axonal mitochondria content. Hum Mol Genet. 2007; 16(22):2720–2728. [PubMed: 17725983]
33. De Vos KJ, Sheetz MP. Visualization and quantification of mitochondrial dynamics in living animal cells. Methods Cell Biol. 2007; 80:627–682. [PubMed: 17445716]
34. Sommer CA, Stadtfeld M, Murphy GJ, et al. Induced pluripotent stem cell generation using a single lentiviral stem cell cassette. Stem Cells. 2009; 27(3):543–549. [PubMed: 19096035]
35. Abrahamsen G, Fan Y, Matigian N, et al. A patient-derived stem cell model of hereditary spastic paraplegia with SPAST mutations. Dis Model Mech. 2013
36. Orso G, Martinuzzi A, Rossetto MG, et al. Disease-related phenotypes in a Drosophila model of hereditary spastic paraplegia are ameliorated by treatment with vinblastine. J Clin Invest. 2005; 115(11):3026–3034. [PubMed: 16276413]
37. An MC, Zhang N, Scott G, et al. Genetic Correction of Huntington's Disease Phenotypes in Induced Pluripotent Stem Cells. Cell Stem Cell. 2012; 11(2):253–263. [PubMed: 22748967]
38. Brennand KJ, Simone A, Jou J, et al. Modelling schizophrenia using human induced pluripotent stem cells. Nature. 2011; 473(7346):221–225. [PubMed: 21490598]
39. Cooper O, Seo H, Andrabi S, et al. Pharmacological rescue of mitochondrial deficits in iPSC-derived neural cells from patients with familial Parkinson's disease. Sci Transl Med. 2012; 4(141): 141ra190.
40. Dimos JT, Rodolfa KT, Niakan KK, et al. Induced pluripotent stem cells generated from patients with ALS can be differentiated into motor neurons. Science. 2008; 321(5893):1218–1221. [PubMed: 18669821]
41. Egawa N, Kitaoka S, Tsukita K, et al. Drug screening for ALS using patient-specific induced pluripotent stem cells. Sci Transl Med. 2012; 4(145):145ra104.
42. Lee G, Papapetrou EP, Kim H, et al. Modelling pathogenesis and treatment of familial dysautonomia using patient-specific iPSCs. Nature. 2009; 461(7262):402–406. [PubMed: 19693009]
43. Marchetto MC, Carromeu C, Acab A, et al. A model for neural development and treatment of Rett syndrome using human induced pluripotent stem cells. Cell. 2010; 143(4):527–539. [PubMed: 21074045]
44. Park IH, Arora N, Huo H, et al. Disease-specific induced pluripotent stem cells. Cell. 2008; 134(5): 877–886. [PubMed: 18691744]
45. Soldner F, Hockemeyer D, Beard C, et al. Parkinson's disease patient-derived induced pluripotent stem cells free of viral reprogramming factors. Cell. 2009; 136(5):964–977. [PubMed: 19269371]
46. Marchetto MC, Gage FH. Modeling brain disease in a dish: really? Cell Stem Cell. 2012; 10(6): 642–645. [PubMed: 22704498]
47. Arlotta P, Molyneaux BJ, Chen J, et al. Neuronal subtype-specific genes that control corticospinal motor neuron development in vivo. Neuron. 2005; 45(2):207–221. [PubMed: 15664173]
48. Falnikar A, Baas PW. Critical roles for microtubules in axonal development and disease. Results Probl Cell Differ. 2009; 48:47–64. [PubMed: 19343314]
49. Fukushima N, Furuta D, Hidaka Y, et al. Post-translational modifications of tubulin in the nervous system. J Neurochem. 2009; 109(3):683–693. [PubMed: 19250341]
50. Palazzo A, Ackerman B, Gundersen GG. Cell biology: Tubulin acetylation and cell motility. Nature. 2003; 421(6920):230. [PubMed: 12529632]
51. Baas PW, Black MM. Individual microtubules in the axon consist of domains that differ in both composition and stability. J Cell Biol. 1990; 111(2):495–509. [PubMed: 2199458]
52. Dompierre JP, Godin JD, Charrin BC, et al. Histone deacetylase 6 inhibition compensates for the transport deficit in Huntington's disease by increasing tubulin acetylation. J Neurosci. 2007; 27(13):3571–3583. [PubMed: 17392473]
53. Outeiro TF, Kontopoulos E, Altmann SM, et al. Sirtuin 2 inhibitors rescue alpha-synuclein-mediated toxicity in models of Parkinson's disease. Science. 2007; 317(5837):516–519. [PubMed: 17588900]

54. Morfini GA, Burns M, Binder LI, et al. Axonal transport defects in neurodegenerative diseases. J Neurosci. 2009; 29(41):12776–12786. [PubMed: 19828789]
55. Sharp DJ, Ross JL. Microtubule-severing enzymes at the cutting edge. J Cell Sci. 2012; 125(Pt 11): 2561–2569. [PubMed: 22595526]
56. Baas PW, Qiang L. Neuronal microtubules: when the MAP is the roadblock. Trends Cell Biol. 2005; 15(4):183–187. [PubMed: 15817373]
57. Millecamps S, Julien JP. Axonal transport deficits and neurodegenerative diseases. Nat Rev Neurosci. 2013; 14(3):161–176. [PubMed: 23361386]
58. Hafezparast M, Klocke R, Ruhrberg C, et al. Mutations in dynein link motor neuron degeneration to defects in retrograde transport. Science. 2003; 300(5620):808–812. [PubMed: 12730604]
59. Puls I, Jonnakuty C, LaMonte BH, et al. Mutant dynactin in motor neuron disease. Nat Genet. 2003; 33(4):455–456. [PubMed: 12627231]
60. Zhao X, Alvarado D, Rainier S, et al. Mutations in a newly identified GTPase gene cause autosomal dominant hereditary spastic paraplegia. Nat Genet. 2001; 29(3):326–331. [PubMed: 11685207]
61. Park SH, Zhu PP, Parker RL, et al. Hereditary spastic paraplegia proteins REEP1, spastin, and atlastin-1 coordinate microtubule interactions with the tubular ER network. J Clin Invest. 2010; 120(4):1097–1110. [PubMed: 20200447]
62. Montenegro G, Rebelo AP, Connell J, et al. Mutations in the ER-shaping protein reticulon 2 cause the axon-degenerative disorder hereditary spastic paraplegia type 12. J Clin Invest. 2012; 122(2): 538–544. [PubMed: 22232211]
63. Kola I, Landis J. Can the pharmaceutical industry reduce attrition rates? Nat Rev Drug Discov. 2004; 3(8):711–715. [PubMed: 15286737]

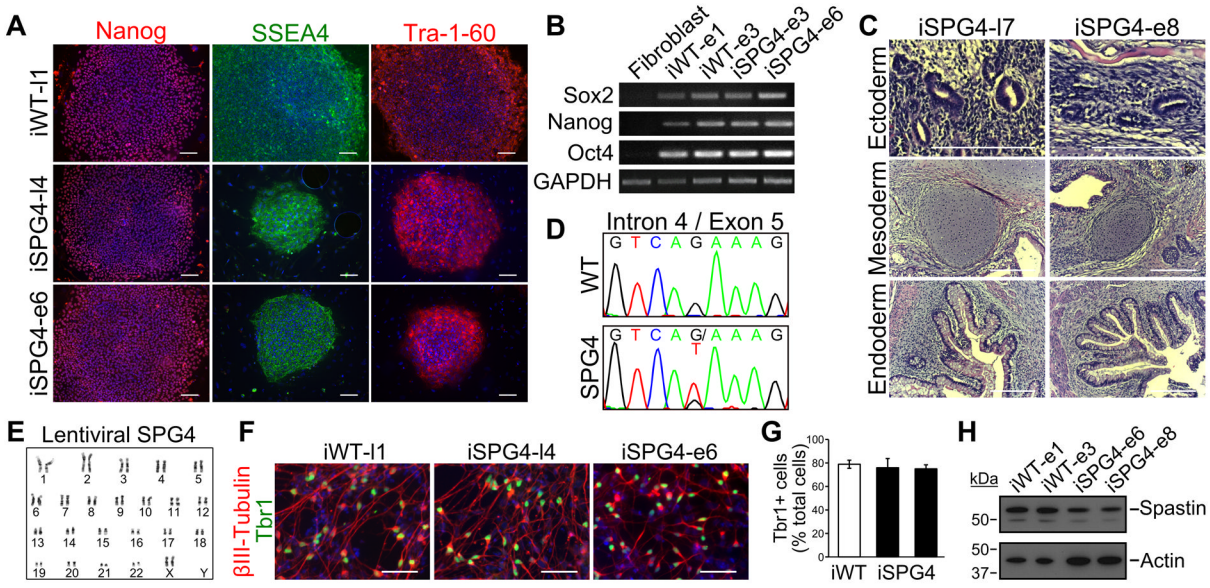

Figure 1.

Characterization and differentiation of SPG4 iPSCs. **(A)** Control (iWT-l1, lentiviral) and SPG4 iPSC lines expressed the hESC markers Tra-1-60, Nanog and SSEA-4. Scale bars: 100 μm. **(B)** Analysis of pluripotency genes in generated iPSC lines (iWT-e1, iWT-e3, iSPG4-e3, iSPG4-e6, episomal) by RT-PCR. **(C)** Hematoxylin and eosin staining of teratoma sections that were derived from iPSCs. Tissues from each germ layer were formed. Scale bars: 200μm. **(D)** Sequencing results confirmed the presence of the intron 4 splice acceptor mutation (c.683-1G>T), which was not found in control cells. **(E)** The lentiviral SPG4 lines maintained a normal 46,XX female karyotype after 10 passages as shown by G-banded analysis. **(F)** The iPSCs were able to efficiently generate telencephalic glutamatergic neurons, as shown by staining for Tbr1. Scale bars: 50μm. **(G)** Percentages of cells immunostained positive for Tbr1 in control (iWT-l1) and SPG4 lines (iSPG4-l4 and iSPG4-l7). Data presented as mean ±SD. **(H)** Western blot analysis revealed a significant decrease in spastin protein in post-mitotic neurons derived from SPG4 iPSCs compared to control neurons. Nuclei are labeled with Hoechst (blue) in A and F.

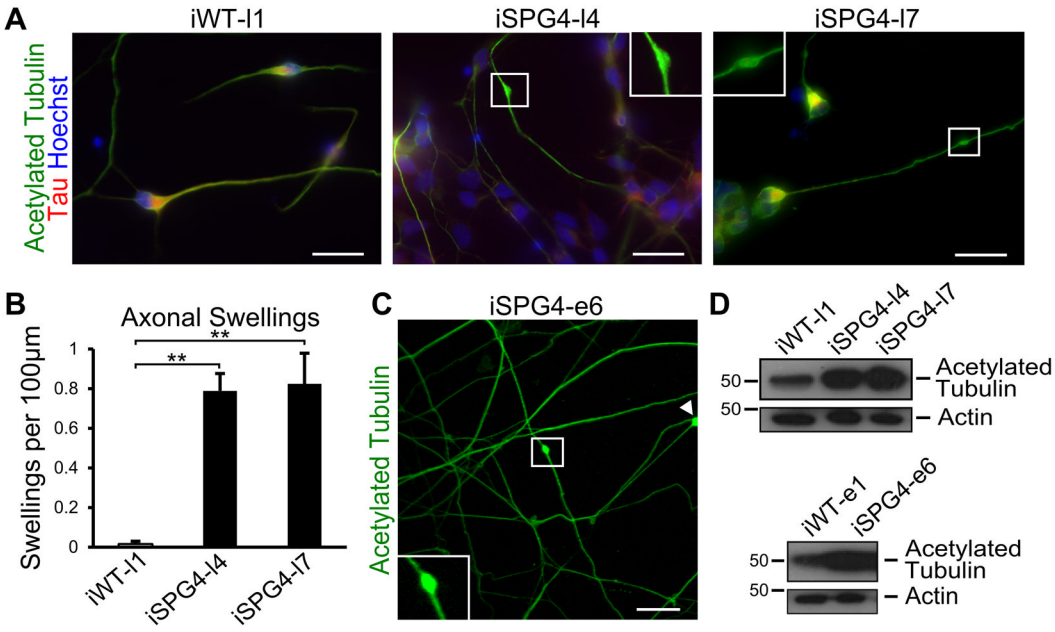

Figure 2.

SPG4 patient-derived neurons display axonal defects. **(A)** Acetylated tubulin staining revealed the presence of swellings along Tau^{+} axons of 6 week-old neurons. Boxed areas are enlarged in insets. **(B)** Quantification revealed a significant increase in axonal swellings in patient-derived neurons compared to control neurons. Data presented as mean ±SD. $^{**}P < 0.01$. **(C)** Episomal SPG4 neurons also possessed axonal swellings. **(D)** Western blots show that acetylated tubulin levels were dramatically increased in the week 6 SPG4-derived neurons compared to controls. Scale bars: 20 μm.

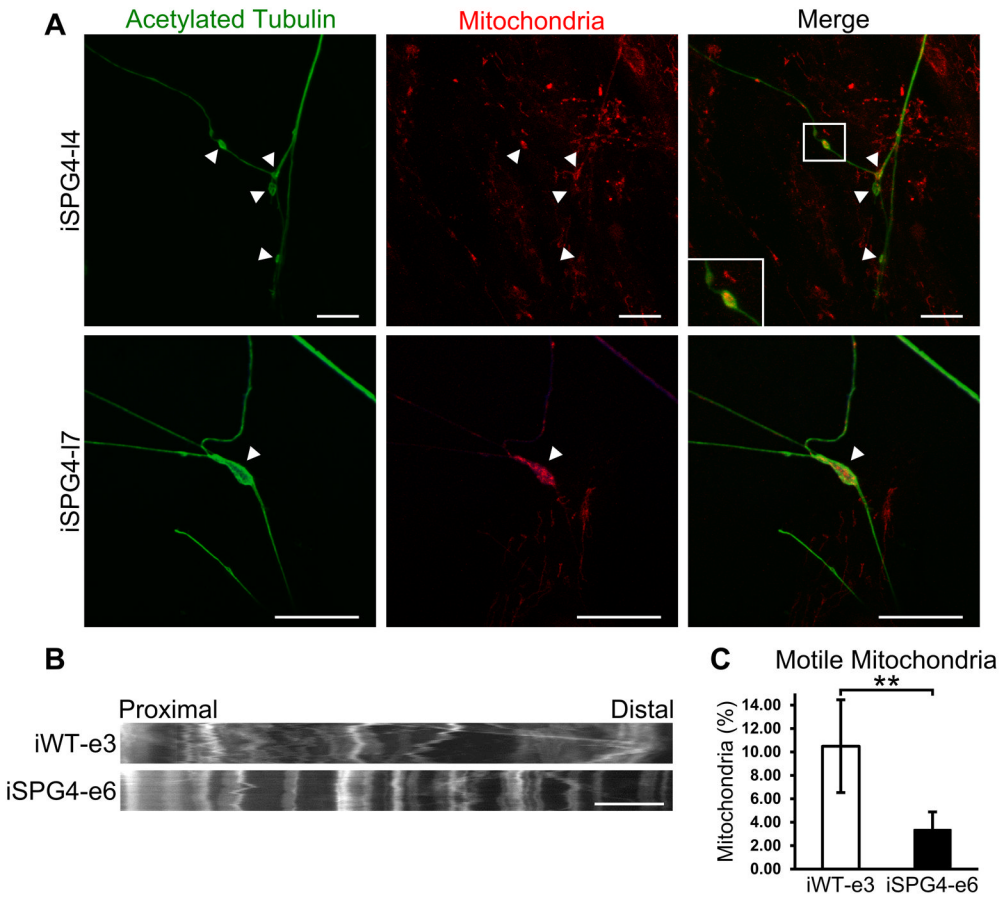

Figure 3.

Disrupted fast axonal transport in SPG4-derived neurons. **(A)** Staining for mitochondria, using MitoTracker Red CMXRos, was enriched within axonal swellings (arrowheads). Scale bars: 20 μm. **(B)** Representative distance versus time kymographs over a 5 minute recording. Scale bar: 10 μm. **(C)** Quantification of motile mitochondria in week 8 forebrain neurons. Data presented as mean ±SD. $^{**}P < 0.01$.

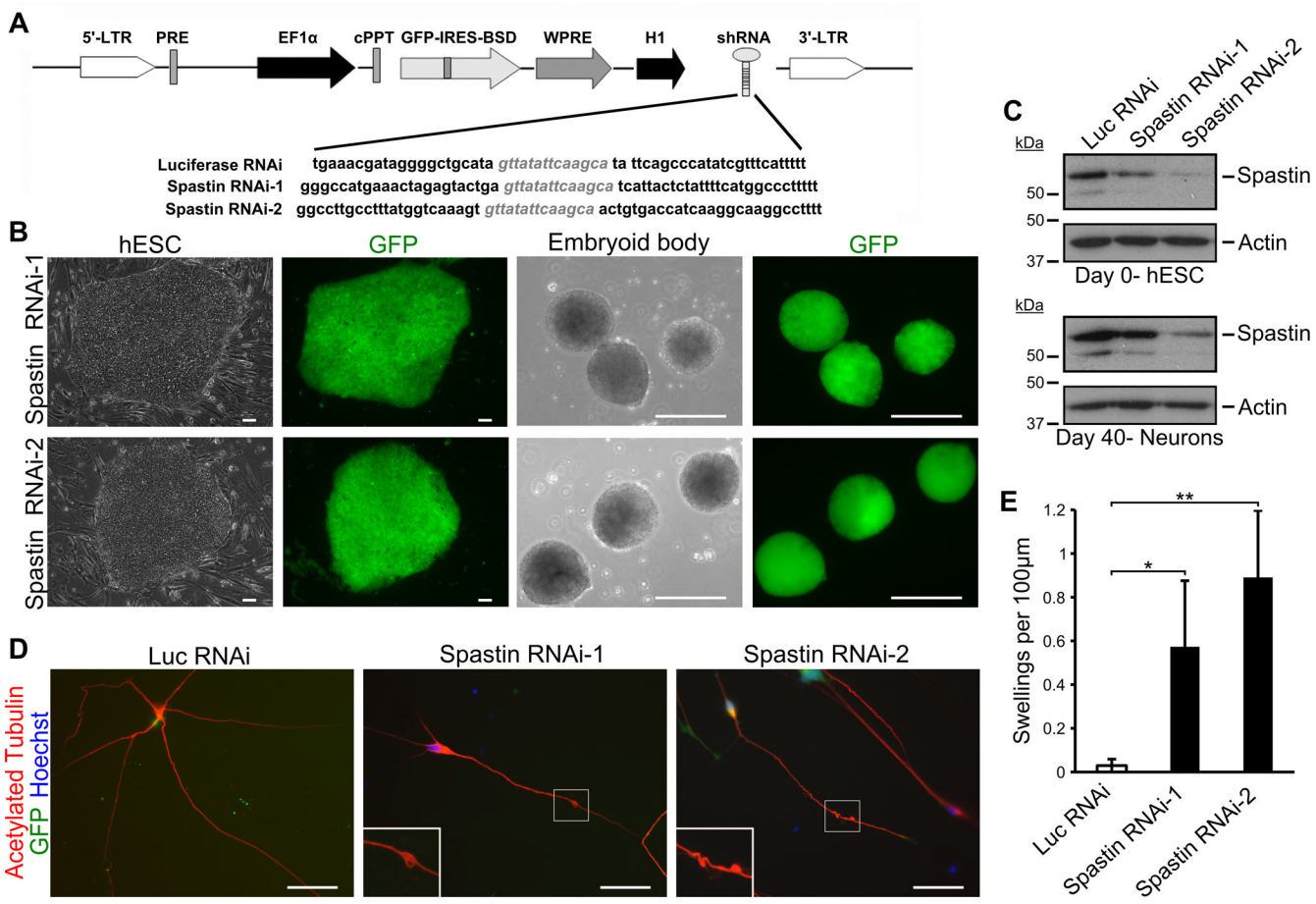

Figure 4.

Spastin knockdown in hESC-derived neurons recapitulates SPG4 patient phenotype. **(A)** Schematic map showing the pLVTHM vector with the shRNA sequence. H9 hESCs were transfected with the indicated lentivirus, and GFP^+ cells were selected. **(B)** hESC colony after lentiviral transfection shows efficient generation of knockdown lines. Expression of shRNA continued during differentiation. Scale bars: 100 µm. **(C)** Western blot analysis confirming knockdown of spastin in both hESCs and neurons after 40 days of differentiation. **(D)** Immunostaining for acetylated tubulin revealed the development of axonal swellings in two spastin RNAi hESC-derived neurons. Hoechst stains the nuclei. Scale bars: 20µm. **(E)** Quantification of axonal swellings shows a significant increase in spastin RNAi-derived neurons compared to control cells. Data presented as mean ±SD. $*P < 0.05$, $**P < 0.01$. Luc, luciferase.

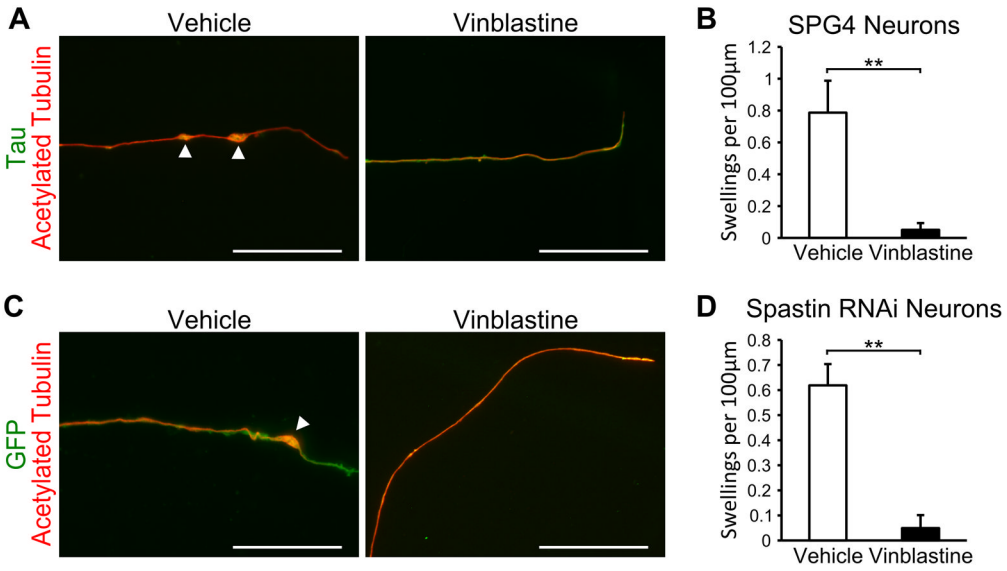

Figure 5.

Vinblastine treatment ameliorates the SPG4 axonal swelling phenotype. **(A)** Week 8 iSPG4-l7 neurons treated with 10 nM vinblastine for 24 hours appeared to have a reduction in axonal swellings compared to control cells, while no deleterious effects were observed. Scale bars: 20µm. **(B)** Quantification revealed that 10 nM vinblastine significantly reduced the number of axonal swellings. **(C)** Treatment with 10 nM vinblastine for 24 hours also reduced axonal swellings in spastin RNAi-1 neurons. Scale bars: 20µm. **(D)** Quantification of axonal swellings in cells treated with vehicle or 10 nM vinblastine. Data presented as mean ±SD. $^{**}P < 0.01$.

Table 1

SPG4-derived neurons have decreased frequency of retrograde fast axonal transport motile events.

	Anterograde Motile Velocity (μm/s)	Retrograde Motile Velocity (μm/s)	Events (>300 nm/s)	Anterograde Events (>300 nm/s)	Retrograde Events (>300 nm/s)
iWT-e3	0.48±0.21	0.50±0.19	0.43±0.09	0.15±0.04	0.29±0.07
iSPG4-e6	0.45±0.12	0.54±0.17	0.14±0.04	0.08±0.02	0.06±0.02
P-value	ns	ns	<0.01	ns	<0.01

The velocity and frequency of mitochondrial motility were quantified in week 8 control and SPG4-derived neurons. No velocity differences were found in either the anterograde or retrograde direction. The frequency of total motile events was significantly decreased in SPG4 neurons. Though there was a non-significant trend toward reduction of anterograde motile events in SPG4 neurons, retrograde events were significantly reduced. Data are presented as means ±SEM. Statistical significance was determined using a two-sided *t*-test.

Stem Cells. Author manuscript; available in PMC 2015 February 01.